

Hydrogen Bonding Mediated by Key Orbital Interactions Determines Hydration Enthalpy Differences of Phosphate Water Clusters

Eliza A. Ruben,[†] Michael S. Chapman,[‡] and Jeffrey D. Evanseck^{*,§}

Institute of Molecular Biophysics, Florida State University, Tallahassee, Florida 32306, Department of Biochemistry & Molecular Biology, School of Medicine, Mail Code L224, Oregon Health Sciences University, 3181 Southwest Sam Jackson Park Road, Portland, Oregon 97239-3098, and Center for Computational Sciences and Department of Chemistry and Biochemistry, Duquesne University, 600 Forbes Avenue, Pittsburgh, Pennsylvania 15282

Received: June 20, 2007

Electronic structure calculations have been carried out to provide a molecular interpretation for dihydrogen phosphate stability in water relative to that of metaphosphate. Specifically, hydration enthalpies of biologically important metaphosphate and dihydrogen phosphate with one to three waters have been computed with second-order Møller–Plesset perturbation and density functional theory (B3LYP) with up to the aug-cc-pvtz basis set and compared to experiment. The inclusion of basis set superposition error corrections and supplemental diffuse functions are necessary to predict hydration enthalpies within experimental uncertainty. Natural bond orbital analysis is used to rationalize underlying hydrogen bond configurations and key orbital interactions responsible for the experimentally reported difference in hydration enthalpies between metaphosphate and dihydrogen phosphate. In general, dihydrogen phosphate forms stronger hydrogen bonds compared to metaphosphate due to a greater charge transfer or enhanced orbital overlap between the phosphoryl oxygen lone pairs, $n(\text{O})$, and the antibonding O–H bond of water. Intramolecular distal lone pair repulsion with the donor $n(\text{O})$ orbital of dihydrogen phosphate distorts symmetric conformations, which improves $n(\text{O})$ and $\sigma^*(\text{O–H})$ overlap and ultimately the hydrogen bond strength. Unlike metaphosphate, water complexed to dihydrogen phosphate can serve as both a hydrogen bond donor and a hydrogen bond acceptor, which results in cooperative charge transfer and a reduction of the energy gap between $n(\text{O})$ and $\sigma^*(\text{O–H})$, leading to stronger hydrogen bonds. This study offers insight into how orbital interactions mediate hydrogen bond strengths with potential implications on the understanding of the kinetics and mechanism in enzymatic phosphoryl transfer reactions.

Introduction

Metaphosphate, PO_3^- , was first proposed as a key intermediate in the aqueous hydrolysis of phosphate monoesters on the basis of the independent work by Westheimer and Bunton in 1955.^{1,2} Owing to the importance of phosphate hydrolysis to biology, the mechanistic role of PO_3^- in the hydrolysis of phosphate monoesters and other related reactions in solution has since been the subject of intense scrutiny, giving way to much experimental and theoretical research.^{3–11} Despite extensive studies, several questions remain concerning the nature of PO_3^- compared to other phosphates. Specifically, the difference in stability between PO_3^- and phosphates in water has been well documented by gas-phase hydration experiments using mass spectroscopy^{3,12,13} and computational investigations,^{7,8,14} but a molecular interpretation for this difference in stability remains elusive.

While PO_3^- has been effectively isolated in the gas phase, in clusters with up to three water molecules, and in aprotic media, the isolation of PO_3^- in aqueous solution has been difficult.¹⁵ Phosphates on the other hand are stable in solution,¹⁶

which is an important biological property of phosphates, as it allows the compounds to be conveniently utilized for energy storage. Energy release through hydrolysis or phosphoryl transfer occurs only after exposure to an enzyme's catalytic site.¹⁷ The differences in hydrogen bonding between dihydrogen phosphate, H_2PO_4^- , and PO_3^- with water molecules may be a key molecular factor in explaining the observed stability differences.

Experimental gas-phase hydration studies have shown that H_2PO_4^- is stabilized by 1.1 kcal/mol over its PO_3^- counterpart in one-water complexes (Scheme 1).^{3,12,13} This trend in stability follows as more water molecules are added. Disagreement between experiment and computation results for the third hydration step of PO_3^- , where the computed enthalpy of hydration (-7.5 kcal/mol) for the third step is significantly less exothermic than reported by experiment (-16.3 kcal/mol).^{7,8,14}

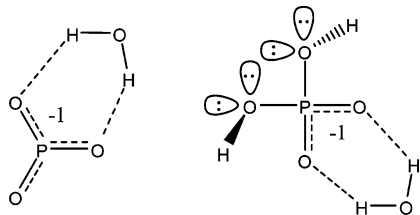
Water clusters of H_2PO_4^- display more exothermic enthalpies of hydration than PO_3^- .^{3,12,13} This is unusual, since anionic oxygens are expected to form stronger hydrogen bonds with water.^{18–20} H_2PO_4^- has only two unprotonated oxygen atoms ready to accommodate one double-hydrogen-bond-donating water molecule, as shown by Scheme 1. On the other hand, PO_3^- has three possible locations, so the addition of two and three water molecules should be more favorable than for H_2PO_4^- . However, this is not observed by experiment. Thus, water clusters of H_2PO_4^- and PO_3^- are ideal candidates to

* To whom correspondence should be addressed. E-mail: evanseck@duq.edu.

[†] Florida State University.

[‡] Oregon Health Sciences University.

[§] Duquesne University.

SCHEME 1: Single-Water Complexes of Metaphosphate (Left, C_{2v}) and Dihydrogen Phosphate (Right, C_1)^a

^a Hydrogen bonding illustrates the double-donor, double-acceptor interactions and distal lone pairs of interest.

examine how orbital interactions can explain relative stabilities and hydrogen-bonding differences.

Independent theoretical studies using MP2/6-31+G(d,p),⁸ CCSD/DZP+,⁷ and B3LYP/6-311++G(d,p)¹⁴ levels of theory have been performed for the complexation of PO_3^- and H_2PO_4^- with water molecules. It was found that PO_3^- and PO_4^- formed low-energy, bifurcated (double-donor, double-acceptor), and symmetric complexes with a single water molecule. Computed enthalpies and free energies of hydration from the reports are consistent with experimental values. However, the studies did not uncover the underlying reasons why PO_3^- and phosphates differ in their interaction with water.

Recent experimental data, such as the red-shift of infrared X–H stretching modes during hydrogen bond formation,²¹ chemical shifts and J couplings in enzyme substrate complexes,²² and X-ray investigations into hydrogen bonds in ice,²³ have suggested that hydrogen bonds involve partial covalent character. The macromolecular refinement of X-ray data is also indicative of a significant covalent component in many biological environments.^{24,25} In recent years, natural bond orbital (NBO) analysis has been increasingly used to quantify the magnitude of electron delocalization (hyperconjugation) describing the partial covalency of hydrogen bonds. NBO studies have been used successfully to explain the origin of hydrogen bond NMR J couplings in DNA binding,²⁶ hydroperoxy radicals binding to water surfaces,²⁷ the electronic basis of improper hydrogen bonds,²⁸ and the origin of strong hydrogen bonds.²⁹ In the NBO methodology, the partial covalency of the hydrogen bond is described by $n(\text{lone pair}) \rightarrow \sigma^*(\text{antibonding orbitals})$ hyperconjugation.³⁰ The magnitude of the $n(\text{lone pair}) \rightarrow \sigma^*(\text{antibonding orbitals})$ interaction presents a quantitative assessment of the hydrogen bond strength. Motivation to use NBO in this work stems from the need to explain subtle differences in hydrogen bonding for one-water complexes and interpret the unusual asymmetric and strong hydrogen bonds between two or more waters with phosphates. The reported hydration enthalpies cannot be easily explained by electrostatic arguments and require a detailed investigation of the individual hydrogen bond interactions.

Due to the physiological importance of phosphates and lack of understanding of how phosphates interact with water, a systematic study of the hydrogen bond strength and its relationship to the stereoelectronic structure of PO_3^- and H_2PO_4^- and observed hydration enthalpies has been undertaken. Electronic structure methods with a variety of basis sets and NBO analysis provide the necessary atomistic and stereoelectronic detail to identify and quantify the origin of differences in hydration enthalpy between PO_3^- and H_2PO_4^- with up to three water molecules. Specifically, $n(\text{O}) \rightarrow \sigma^*(\text{O–H})$ hyperconjugation, or partial covalency, is probed to evaluate differences in

hydrogen bonding between the phosphates. Central to this work is the relationship found between phosphate conformation, hydrogen-bonding configurations, $n(\text{O})$ and $\sigma^*(\text{O–H})$ orbital overlap, charge transfer magnitude, hydrogen-bonding strength, and ultimately reported hydration enthalpy difference. It is crucial to achieve an understanding of how phosphates interact with water on such an elementary basis before the influence of solvent and pH upon phosphoryl-transfer reactions may be better understood.

Methods

All electronic structure calculations were carried out with the Gaussian program.³¹ The computational resources were provided by the School of Computational Science and Information Technology (CSIT) at Florida State University and the Center for Computational Sciences (CCS) at Duquesne University.

The electronic description of hydrogen bonding between phosphates and water requires a careful choice of the method and basis set.³² To incorporate the effects of electron correlation, the energy-minimized structures were located with the density functional (DFT) and second-order Møller–Plesset many-body perturbation (MP2) theories.³³ Specifically, DFT was implemented with Becke’s three-parameter hybrid (exchange) functional^{34,35} with the correlation functional provided by Lee, Yang, and Parr (B3LYP).³⁶ Due to the inability of DFT methods to describe dispersive forces,^{37–39} MP2 optimizations were carried out on all structures to serve as a point of verification and test of DFT.

The addition of diffuse functions is imperative to describe the spatial distribution of the phosphate anion accurately.^{40,41} However, if large numbers of diffuse functions are used, then there is a potential of extra electrons “escaping”.⁴² Thus, the influence of diffuse functions on the anions was evaluated. In addition, an adequate description of polarization is crucial, since it has been shown that p-polarization functions on the hydrogen atoms are important for a variety of hydrogen-bonding systems.^{43–46} Consequently, 20 basis sets,^{40,47–53} as shown in Table S1 of the Supporting Information, were chosen to evaluate the energetic convergence of the electronic structure studies.

Basis set superposition errors (BSSEs) were obtained using the Boys–Bernardi counterpoise correction method.⁵⁴ In prior theoretical calculations of gas-phase hydration energies of PO_3^- , BSSE errors were not considered.^{7,8,14} It has been argued that BSSE is not necessary, since there is a consistent cancellation between the effects of basis set incompleteness and electron correlation.⁷ It has been reported that the inclusion of BSSE shifts computed thermodynamic parameters away from experimental values.⁷ In fact, some researchers have concluded that only half of the effects from BSSE should be included.⁵⁵ However, it has become increasingly clear that the generalization of BSSE importance is difficult and that its impact depends on the system under investigation and the level of theory implemented.

Contributions due to thermal, vibrational, rotational, and translational motions, including zero-point energies, were included separately by standard statistical mechanical procedures available in Gaussian. Frequency analysis was used to characterize all stationary points as minima and provide thermodynamic and zero-point energy corrections at 298 K.⁵⁶

Natural bond orbital (NBO)⁵⁷ analysis was performed using the NBO 3.1 program interfaced into the Gaussian program. NBO transforms the nonorthogonal atomic orbitals from the

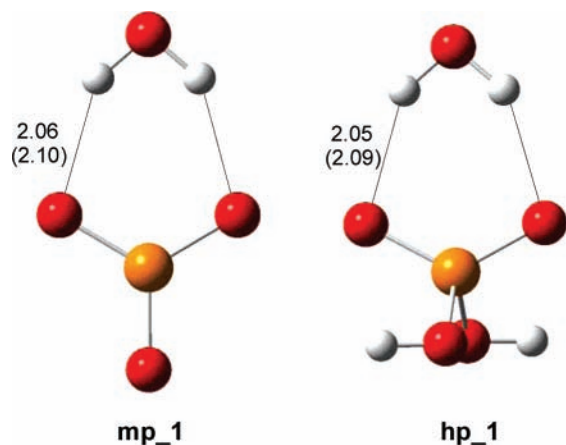


Figure 1. Optimized geometries of metaphosphate (**mp_1**) and dihydrogen phosphate (**hp_1**) complexes with one water at the MP2/6-311++G(3df,2p) level. Hydrogen bond lengths are given for MP2/6-311++G(3df,2p) and B3LYP/6-311++G(3df,2p) in parentheses. Bond lengths are in angstroms. Oxygen is represented by the color red, phosphorus by orange, and hydrogen by white.

wave function into natural atomic orbitals (NAOs), natural hybrid orbitals (NHOs), and natural bond orbitals, each of which are complete and orthonormal. This allows electron density to be treated in a more intuitive manner, i.e., localized onto bonds

and atoms, leading to a better description of the molecule as a localized Lewis structure. In effect, NBO transformation provides filled orbitals that are more concentrated (localized) in terms of occupancies. This then allows delocalizing interactions to be treated as a perturbation through second-order perturbation theory. The $E(2)$ energy values from the second-order perturbation method then provide a reasonable quantitative description of the magnitude of such delocalizing interactions.^{58,59}

The NBO method has been cited for overestimating charge transfer effects^{60,61} compared to other methods of decomposing ab initio intermolecular interaction energies. The latter include the Kitaura and Morokuma (KM)⁶² and block-localized wave function^{63,64} methods. For the water dimer, charge transfer estimates by the KM and NBO methods are -1.8^{65} and -9.3^{66} kcal/mol. It has been noted that NBO analysis stresses the role of orbital interaction between filled and unfilled orbitals, whereas the KM analysis emphasizes classical electrostatics from overlapping charge distributions.^{67,68} In the application reported here, neither an overestimation by NBO nor underestimation by other methods is critical, because the errors will approximately cancel when relative differences are examined. Indeed the similarity of charge transfer trends between NBO and block-localized wave function calculations has been previously noted.⁶⁸

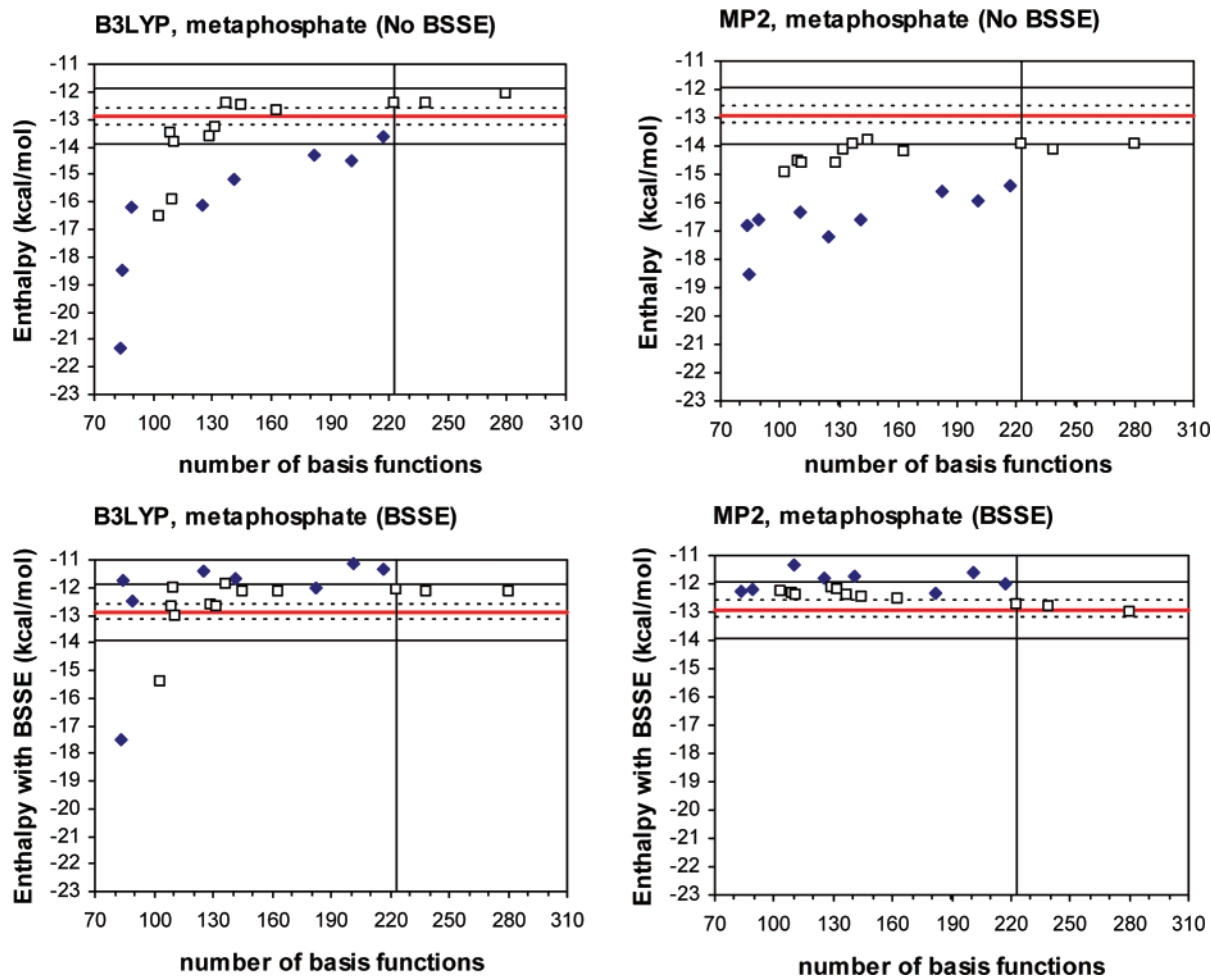


Figure 2. Hydration enthalpies versus number of basis functions for the first hydration step of metaphosphate. The experimental enthalpy is given as a solid line in red, and calculated values are given as filled tilted squares (polarization, no diffuse functions) and open squares (polarization and diffuse functions). Vertical lines indicate the 6-311++G(3df,2p) basis set at 223 basis functions selected in this study to represent a converged level of theory. Experimental errors were reported at 0.33 kcal/mol, and the bars are represented as dashed horizontal lines. A reference of 1 kcal/mol is given by solid horizontal lines.

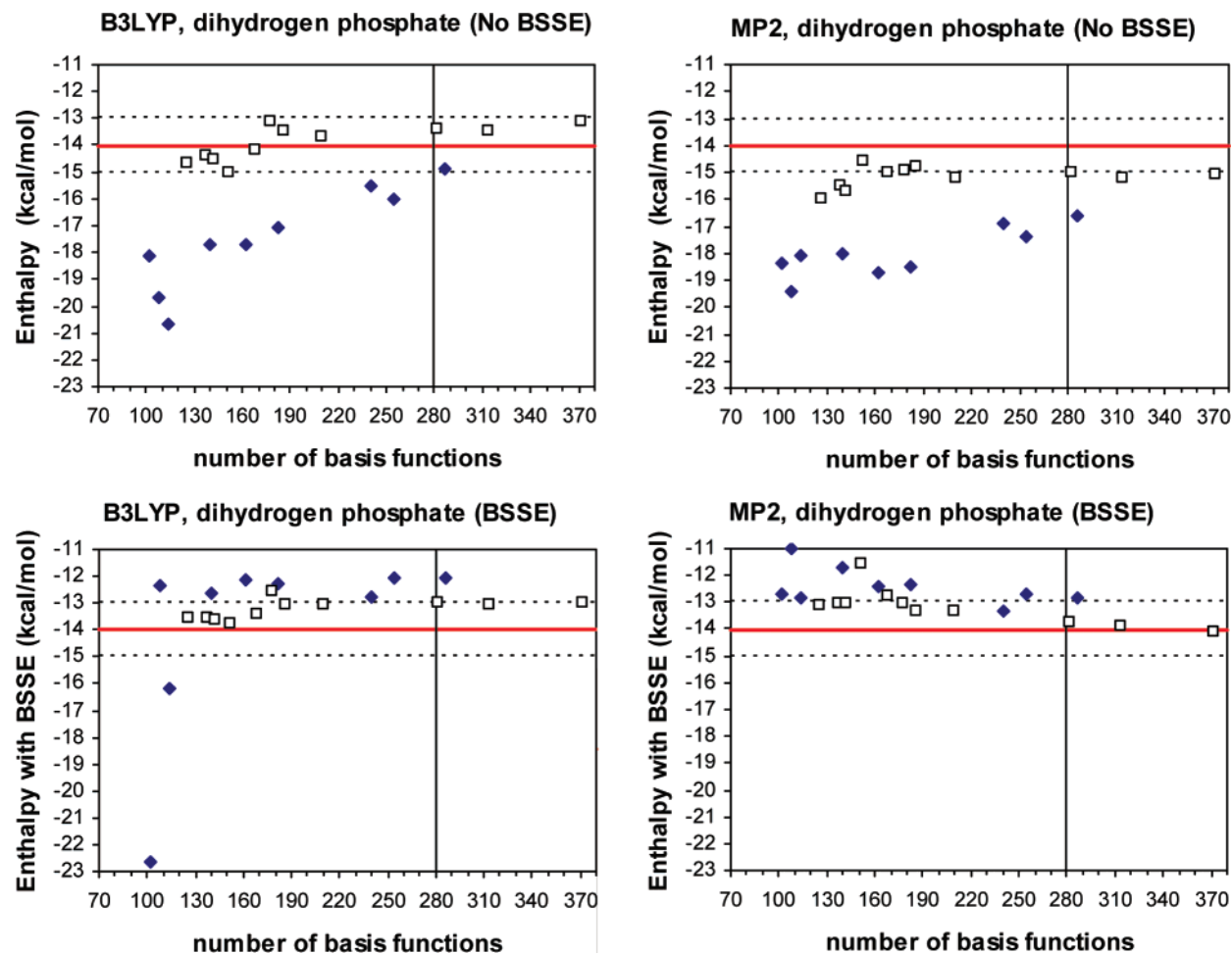
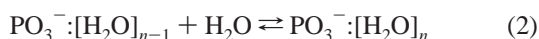
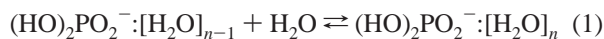


Figure 3. Hydration enthalpies versus basis functions for the first hydration step of dihydrogen phosphate. The experimental value is given in red, and calculated values are given as filled tilted squares (polarization, no diffuse functions) and open squares (polarization and diffuse functions). Vertical lines indicate the 6-311++G(3df,2p) basis set at 280 basis functions selected for this study to represent a converged level of theory. Experimental errors were reported at 1 kcal/mol and are represented by dashed horizontal lines.

The calculation of interaction enthalpies was done according to the equilibrium reaction used in previous enthalpy of hydration studies for H_2PO_4^- in eq 1 and PO_3^- in eq 2 with $n = 1-3$.^{7,8}



Results and Discussion

The main aim of this work is to understand the difference in the experimentally reported gas-phase hydration enthalpies between PO_3^- and H_2PO_4^- with one to three waters.^{7,8,13,69} In particular, the examination of the structural and energetic relationship of the hydrogen bonds formed by different phosphates with water is a crucial first step toward the accurate description of phosphate solvation and reactivity. In this work, a two-step approach has been used to investigate hydrogen bonding in PO_3^- and H_2PO_4^- . First, the ability of different levels of theory to reproduce the experimentally determined hydration enthalpies for one-water complexes was evaluated. Such studies were used to identify the level of theory needed to converge upon the experimental hydration enthalpy so that similar approaches could be used with larger two- and three-water systems. Second, NBO analysis was utilized to

forge a link among subtle structural changes, stereoelectronic effects, and the strength of hydrogen bonding at the level of theory producing hydration enthalpies converged to experiment.

Assessment of Methods and Basis Sets with One-Water Phosphate Complexes. Multiple starting orientations between the phosphates and a single water resulted in energy-minimized bifurcated complexes, as shown in Figure 1. As with other theoretical studies, bifurcated complexes were identified as the lowest energy stationary points.^{7,8,14} When water was a hydrogen bond acceptor for the hydroxyl group of H_2PO_4^- , the hydration enthalpy for the single-water complex was ~ 30 kcal/mol higher, so this configuration was not considered further.

The complexation of a single water molecule with PO_3^- and H_2PO_4^- was computed at several levels of theory to choose one that can reproduce experimental enthalpies of hydration reported by gas-phase high-pressure mass spectroscopy^{12,13} and electrospray mass spectrometry.³ Two methods, B3LYP and MP2, in conjunction with up to 16 different Pople style basis sets and four Dunning correlation-consistent basis sets were used to test the incorporation of different functions on heavy and light atoms. The numbers of basis functions of PO_3^- and H_2PO_4^- and interaction enthalpies of the bifurcated complexes at the various levels of theory are given in Table S1. Plots of the computed hydration enthalpy as a function of the number

TABLE 1: Covalent Contribution to Hydrogen-Bonding Interactions between Metaphosphate and Dihydrogen Phosphate^a

	MP2/6-311++G(3cf,2p)		B3LYP/6-311++G(3df,2p)	
	H ₂ PO ₄ ⁻	PO ₃ ⁻	H ₂ PO ₄ ⁻	PO ₃ ⁻
<i>E</i> (2) (kcal/mol)				
n(O) → σ*(O–H) 1	3.74	13.89	2.88	3.43
n(O) → σ*(O–H) 2	1.01	0.85	0.85	0.74
n(O) → σ*(O–H) 3	0.58		0.83	
total <i>E</i> (2) (kcal/mol)	5.33	4.74	4.56	4.17
total <i>E</i> (2) (kcal/mol) of both H bonds	10.66	9.48	9.12	8.34
percentage of total interaction energy	76.1	72.9	71.0	64.1
total <i>E</i> _{del} (kcal/mol) of both H bonds	9.06	7.89	7.74	6.89
percentage of total interaction energy	64.7	60.6	60.2	58.3

^aNBO energy values were calculated using the HF/6-311++G(3df,2p) wavefunction on the MP2/6-311++G(3df,2p)- and B3LYP/6-311++G(3df,2p)-optimized structures.

TABLE 2: Hydrogen-Bonding Distances in Angstroms for Metaphosphate and Dihydrogen Phosphate with One Water Molecule

	dihydrogen phosphate	metaphosphate
full optimization	2.055	2.064
optimization without n(O) → σ*(O–H) interactions	2.106	2.093

of basis functions used in the calculation both with and without BSSE corrections are shown for PO₃⁻ (Figure 2) and H₂PO₄⁻ (Figure 3).

The reported experimental error in the interaction enthalpy between one water and PO₃⁻ is 0.33 kcal/mol,³ as indicated by the dashed horizontal lines in Figure 2. For visual assistance, a reference of 1 kcal/mol surrounding the experimental value is also given as solid horizontal lines. The experimental error reported for H₂PO₄⁻ was 1 kcal/mol, as indicated by the dashed horizontal lines in Figure 3.¹²

Previously, the effects of BSSE have largely been ignored in understanding the hydration of phosphate systems.^{7,8,14} However, the incorporation of BSSE into the computed hydration enthalpies of these phosphate systems is important to achieve experimental agreement within the reported accuracy, as seen in Figures 2 and 3. Without BSSE for PO₃⁻ and H₂PO₄⁻, both MP2 and B3LYP overestimate the enthalpies of hydration by several kilocalories per mole. In general, basis sets that rely only upon increases in polarization without BSSE correction (black tilted squares, top entries of Figures 2 and 3) overestimate the enthalpy of hydration. The inclusion of more extensive polarization functions (without diffuse functions) leads to the improvement of predicted enthalpies of hydration. However, convergence to experimental values is slow using B3LYP and is never attained using MP2. In essence, the additional polariza-

tion does not compensate completely for the incompleteness of the basis set.

In general, basis sets with diffuse functions have a more drastic and rapid impact on the computed enthalpies for both B3LYP and MP2 without BSSE. Basis sets with increases in both diffuse and polarization functions (open squares, top entries of Figures 2 and 3) produce enthalpies of hydration that are within 1 kcal/mol of experiment when using B3LYP (6-31+G(d) and 6-311G(d,p) are the exceptions for PO₃⁻). MP2 without BSSE overestimates the enthalpies by less than 2 kcal/mol consistently across the range of basis sets with diffusion functions. The importance of supplementary functions for the 6-31G(d,p) and 6-311G(d,p) basis sets has been reported⁷⁰ for weakly bound complexes^{71–73} and systems involving lone pair electrons.³

Including BSSE in the computations eradicates the large fluctuations in the computed enthalpies of hydration, as seen in Figures 2 and 3. Improvement in the predicted hydration enthalpies is seen for most levels of theory. The 6-311++G(3df,2p) basis set was selected, since it produced hydration enthalpies within experimental error and gives virtually identical enthalpies compared to two smaller and two larger basis sets including diffuseness. The basis set chosen delivers experimental accuracy and computational economy of resources. In particular, BSSE brings the computed MP2/6-311++G(3df,2p) into excellent agreement with experiment. The hydration enthalpy of PO₃⁻ with one water molecule is computed to be -12.7 kcal/mol (-12.9 kcal/mol from experiment),¹² whereas that of H₂PO₄⁻ is computed to be -13.9 kcal/mol (-14.0 kcal/mol from experiment).^{3,12} The impact of BSSE is less on B3LYP energies than on MP2 energies. However, BSSE has a tendency to overcorrect B3LYP energies. The computed B3LYP/6-

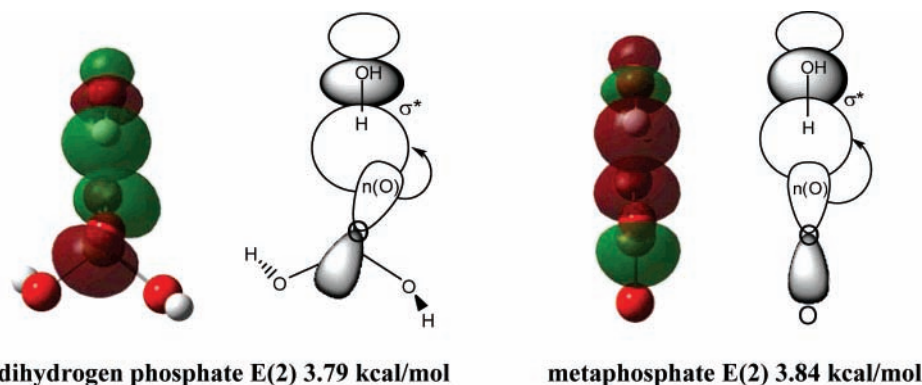


Figure 4. Top view of one-water complexes with the phosphates illustrating the primary n(O) → σ*(O–H) head-to-head interaction between dihydrogen phosphate and metaphosphate with water. For each system, the left-hand figure shows the computed orbitals and the right-hand side is a schematic view.

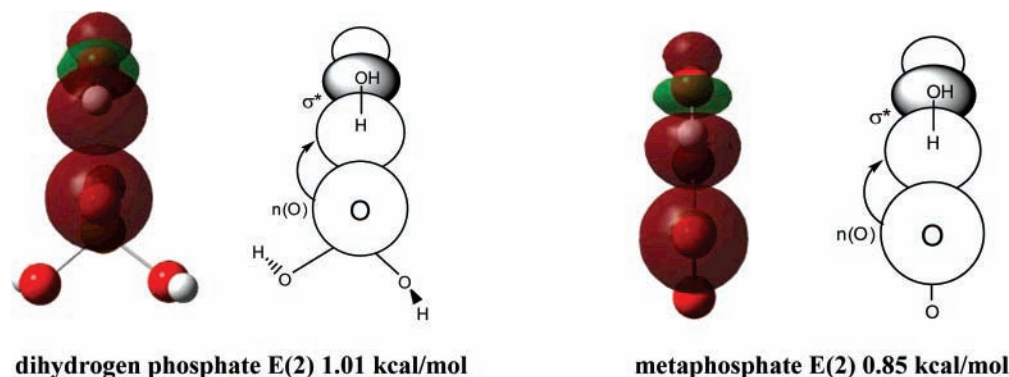


Figure 5. Top view of one-water complexes with the phosphates illustrating the secondary $n(\text{O}) \rightarrow \sigma^*(\text{O}-\text{H})$ interaction. This figure highlights the reduced orbital overlap relative to that shown in the previous figure. For each system, the left-hand figure shows the computed orbitals and the right-hand side is a schematic view.

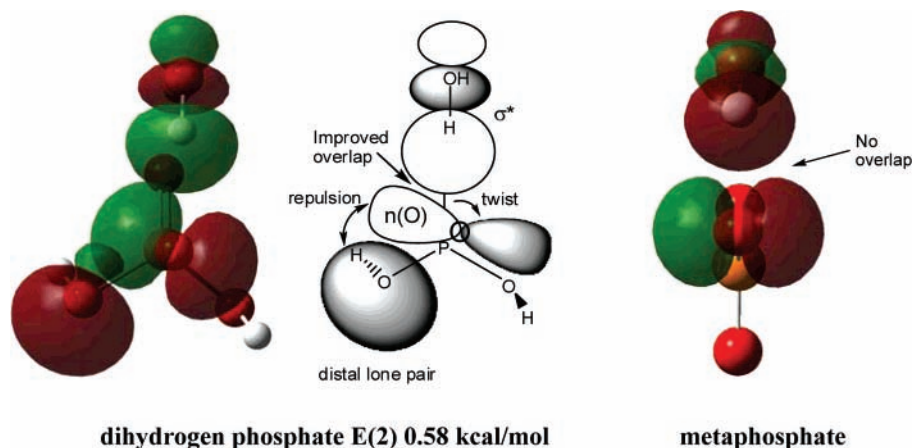


Figure 6. Top view of one-water complexes with the phosphates illustrating the tertiary $n(\text{O}) \rightarrow \sigma^*(\text{O}-\text{H})$ interaction present in dihydrogen phosphate but absent in metaphosphate. For each system, the left-hand figure shows the computed orbitals and the right-hand side is a schematic view.

311++G(3df,2p) hydration enthalpies give slightly better agreement with experiment when basis set superposition is not included.

Orbital Interactions and Hydrogen Bond Strength of PO_3^- and H_2PO_4^- with One Water. NBO analysis results in two main hyperconjugative $n(\text{O}) \rightarrow \sigma^*(\text{O}-\text{H})$ interactions responsible for each hydrogen bond in PO_3^- , but three hyperconjugative $n(\text{O}) \rightarrow \sigma^*(\text{O}-\text{H})$ interactions responsible for each hydrogen bond in H_2PO_4^- , as shown in Table 1. The sum of these interactions indicates that hydrogen bonding is stronger in H_2PO_4^- , as compared to PO_3^- , by 1.3 kcal/mol. To verify the results, deletion energies place this value at 1.2 kcal/mol, a value in good agreement with the experimental difference (1.1 kcal/mol) between enthalpies of PO_3^- and H_2PO_4^- when complexed with one water molecule.⁷⁴

As a percentage of total interaction energies, the $E(2)$ values for H_2PO_4^- and PO_3^- are 76% and 73%. The experimental values are -14.0 and -12.9 kcal/mol, respectively.^{3,12,13} When using deletion energies, the computed percentage reduces to 65% and 61%, respectively. A value of around 60% is in keeping with general NBO evaluations of charge transfer hydrogen-bonding interactions.⁷⁴ Nevertheless, both the $E(2)$ and deletion methods give hydrogen-bonding, charge transfer, or delocalization energies that are more pronounced in H_2PO_4^- than in PO_3^- .

Energy Minimization of Metaphosphate and Dihydrogen Phosphate with One Water in the Absence of Covalent Interactions. To test the importance of hyperconjugation effects on the hydrogen-bonding differences between H_2PO_4^- and PO_3^-

with one water, energy minimizations were performed with the specific $n(\text{O}) \rightarrow \sigma^*(\text{O}-\text{H})$ interactions removed. In this way, the hydrogen bonds formed should be due to the electrostatic contributions and not partial covalency delivered by hyperconjugation. The hydrogen bond lengths are computed to increase from 2.055 Å (with hyperconjugation) to 2.106 Å (without hyperconjugation) for H_2PO_4^- , while that for PO_3^- increases from 2.064 Å (with hyperconjugation) to 2.093 Å (without hyperconjugation), as shown in Table 2. This emphasizes the importance of hyperconjugation, because only when its effects are considered do the hydrogen bond lengths and presumably strengths correlate with experiment. Reiterating this point, hyperconjugation provides stronger and shorter hydrogen bonds for H_2PO_4^- compared to PO_3^- .

Hydrogen Bond Orbital Interactions of Metaphosphate and Phosphate with One Water Molecule. An analysis of the orbitals in both PO_3^- and H_2PO_4^- shows that both phosphates share a common motif of interactions with water, which include primary (defined by the highest $E(2)$ and E_{del} values) and secondary (defined by the second highest $E(2)$ and E_{del} values) interactions. The primary $n(\text{O}) \rightarrow \sigma^*(\text{O}-\text{H})$ interaction, defined by the charge transfer in both PO_3^- and H_2PO_4^- , arises from the interaction between the lone pair $n(\text{O})$ on the phosphate oxygen and the $\sigma^*(\text{O}-\text{H})$ antibonding orbital of the water directly facing each other, as shown in Figure 4.

The two orbitals are oriented head-to-head, providing strong overlap for the primary mechanism for charge transfer. The secondary $n(\text{O}) \rightarrow \sigma^*(\text{O}-\text{H})$ interaction in both PO_3^- and H_2PO_4^- arises from the charge transfer between a second oxygen

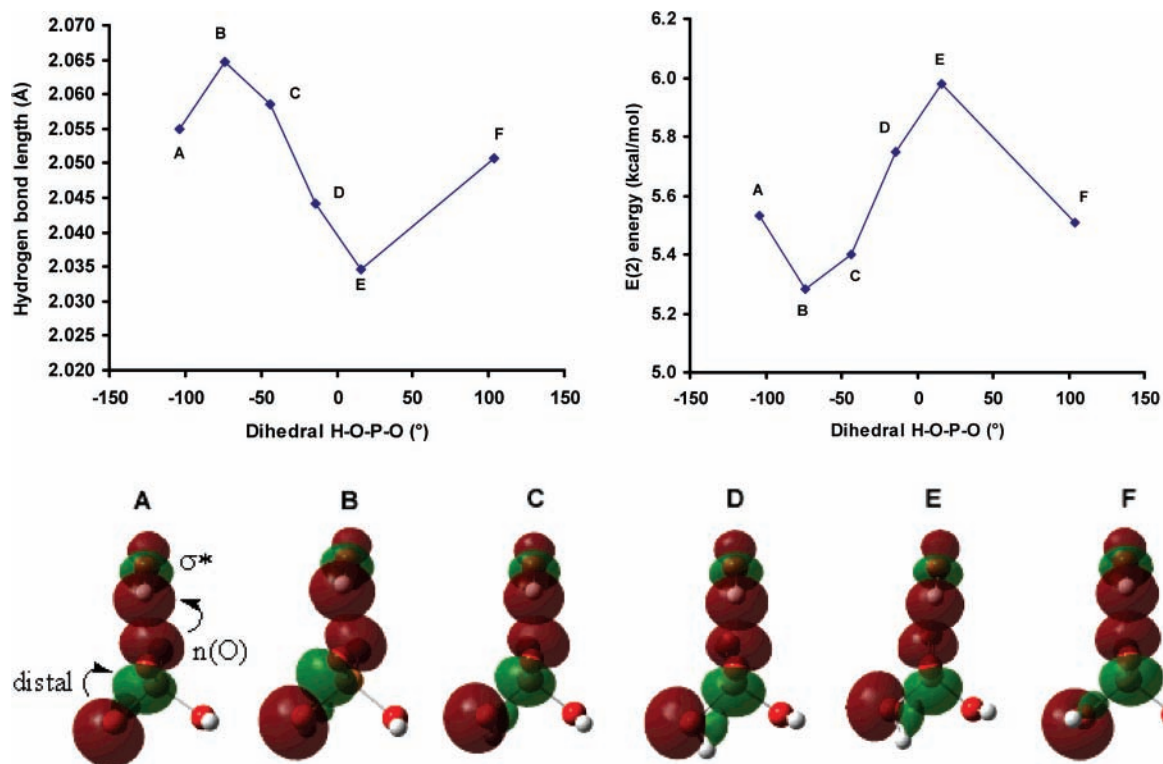


Figure 7. Orientation of orbitals as a function of the systematic change of the H–O–P–O dihedral. The impact of distal lone pair clash is shown to affect $n(\text{O}) \rightarrow \sigma^*(\text{O}-\text{H})$ collinearity. Structure **A** is the final optimized structure. Note that **A** is a local energy minimum, because only one hydrogen bond is being analyzed.

TABLE 3: Hydration Enthalpies of Metaphosphate and Dihydrogen Phosphate at the B3LYP/6-311++G(3df,2p) and MP2/6-311++G(3df,2p) Levels of Theory Corrected for BSSE^a

	$n - 1, n$	calculated ΔH		Expt
		B3LYP	MP2	
metaphosphate, PO_3^-	0, 1	-12.1 (-12.4)	-12.7 (-13.9)	-12.9 ³
	1, 2	-9.8 (-10.6)	-11.4 (-12.2)	-11.4 ³
	2, 3	-7.9 (-9.2)	-7.5 (-10.7)	-16.3 ¹²
dihydrogen phosphate, H_2PO_4^-	0, 1	-13.0 (-13.4)	-13.7 (15.0)	-14.0 ¹²
	1, 2	-11.6 (-12.7)	-11.4 (-14.0)	-12.3 ^{3,12}
	2, 3	-12.5 (-14.2)	-8.8 (-13.6)	

^a Energies not corrected for BSSE are given in parentheses.

lone pair projecting upward and not directly toward the water $\sigma^*(\text{O}-\text{H})$ orbital, as shown in Figure 5. The orientation of the two orbitals provides less overlap, as compared to the primary charge transfer interaction.

The final interaction present in H_2PO_4^- , but absent in PO_3^- , is crucial to understanding the difference in observed hydration enthalpies and stems from donation from an oxygen lone pair almost perpendicular to the water's $\sigma^*(\text{O}-\text{H})$ orbital. When this lone pair is perfectly perpendicular to the $\sigma^*(\text{O}-\text{H})$ orbital, as in the case of PO_3^- , no interaction occurs because both constructive and destructive orbital contributions cancel, as shown in Figure 6.

In the case of H_2PO_4^- , the donor oxygen lone pair is tilted by $\sim 25^\circ$, which is sufficient to allow for orbital overlap and promote charge transfer, as shown in Figure 6. It is computed that the distal lone pair from the hydroxyl substituent clashes with the donor $n(\text{O})$ orbital and causes a distortion that twists the donor lone pair away from the symmetry plane. This is not possible in PO_3^- . The new $n(\text{O})$ orientation creates orbital overlap between the $n(\text{O})$ and $\sigma^*(\text{O}-\text{H})$ orbitals, resulting in stronger charge transfer and hydrogen bonding in H_2PO_4^- .

To further evaluate the hydrogen bond strength dependency on the position of the distal lone pairs, the dihedral of one

hydroxyl substituent (H–O–P–O) was rotated in 30° increments. As seen in Figure 7, the H–O–P–O dihedral dictates the position of the distal lone pairs. As the dihedral is varied, the interaction between the distal lone pair and $n(\text{O})$ changes, which in turn affects the degree of $n(\text{O})$ and $\sigma^*(\text{O}-\text{H})$ overlap (collinearity) and ultimately the hydrogen bond strength.

Starting at a H–O–P–O dihedral of -100° (**A**), a tilt of $\sim 25^\circ$ from collinearity is observed between the $n(\text{O})$ and $\sigma^*(\text{O}-\text{H})$ orbitals. By rotating H–O–P–O by 30° from **A** to **B** (Figure 7), the clash between the remote lone pair and $n(\text{O})$ becomes more intense, resulting in a 35° tilt in collinearity between orbitals. The hydrogen bond length increases by 0.01 Å, and the charge transfer decreases by 0.2 kcal/mol. Continued rotation of H–O–P–O diminishes the interaction between the distal lone pair and $n(\text{O})$, resulting in improved collinearity (**C**–**E**) between $n(\text{O})$ and $\sigma^*(\text{O}-\text{H})$ with shortening of the hydrogen bond and strengthening of charge transfer. Not only does this further validate the previous finding that the hydrogen bond strength depends on the position of distal lone pairs, but also that charge transfer or covalent hydrogen bonding plays a crucial role in hydrogen bond strengths. This finding implies that overall hydration of H_2PO_4^- and PO_3^- depends on the distal lone pair

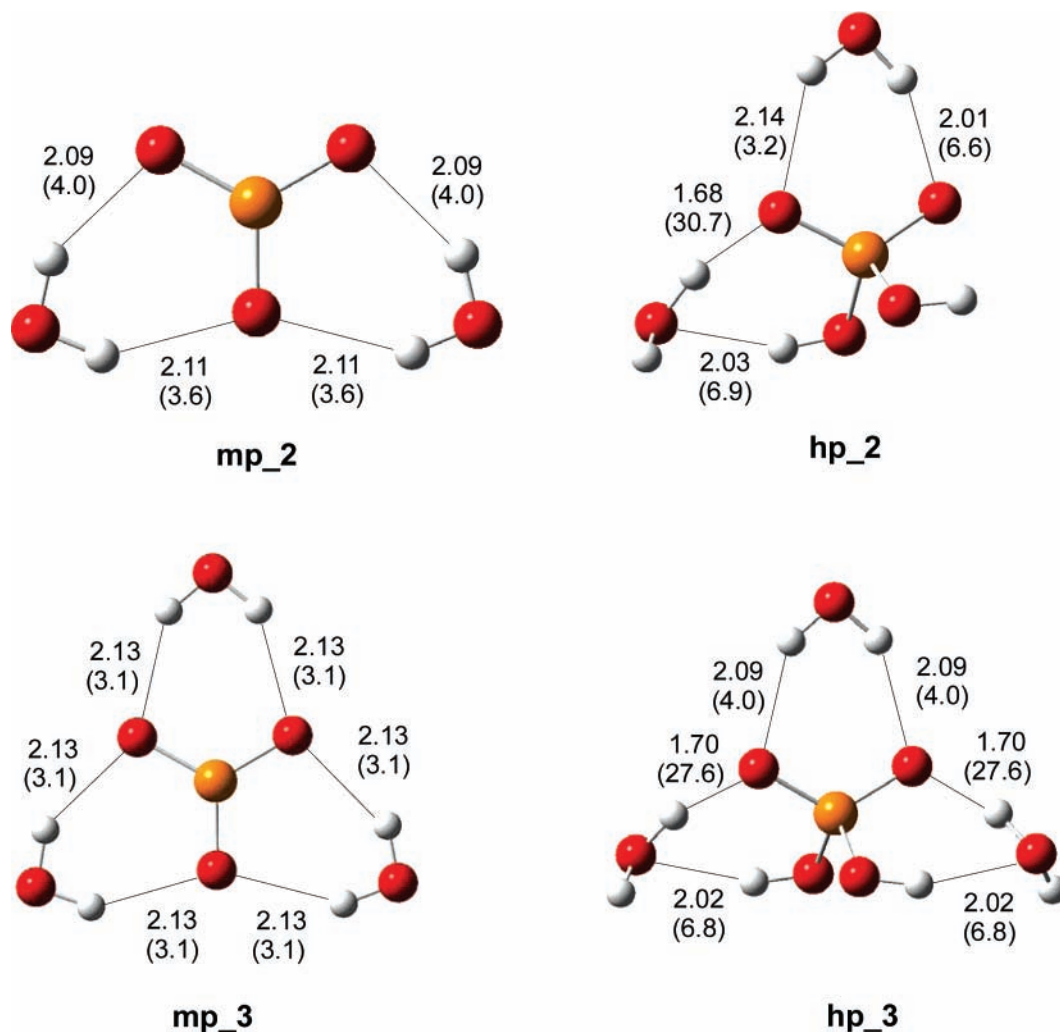


Figure 8. Optimized geometries of metaphosphate (**mp_2** and **mp_3**) and dihydrogen phosphate (**hp_2** and **hp_3**) complexes with two and three waters at the MP2/6-311++G(3df,2p) level, with hydrogen bond lengths in angstroms. $E(2)$ values of the $n(\text{O}) \rightarrow \sigma^*(\text{O}-\text{H})$ interactions in kilocalories per mole are given in parentheses. Oxygen is represented by the color red, phosphorus by orange, and hydrogen by white.

orientation, or in simpler terms, hydration depends on the phosphate conformation.

Geometries and Energies: Two- and Three-Water Complexes of Metaphosphate and Dihydrogen Phosphate. Starting orientations for two- and three-water complexes with PO_3^- were obtained from prior theoretical calculations.^{3,14} Multiple starting orientations were used to search for the low-energy complexes of H_2PO_4^- with two and three water molecules. The lowest energy two-water configuration is different from that reported earlier,⁸ being 1.4 kcal/mol lower in energy using B3LYP/6-311++G(3df,2p). The primary difference between the structure previously reported and the newly calculated one is how the two water molecules hydrogen bond with H_2PO_4^- . The new structure has one water serving as a double hydrogen bond donor to the deprotonated oxygen atoms and one water acting as a simultaneous hydrogen bond donor to a deprotonated oxygen and a hydrogen bond acceptor to a protonated oxygen atom. Both waters in the Houk structure serve as hydrogen bond donors to one protonated and one deprotonated oxygen.⁸ The three-water structure of H_2PO_4^- has not been previously reported. Despite extensive searching, it cannot be ascertained with certainty whether the two- or three-water complexes with H_2PO_4^- are global minima, although the computed hydration enthalpy for the two-water complex is within experimental error.

Interaction enthalpies of PO_3^- and H_2PO_4^- complexes with two- and three-water complexes at the B3LYP/6-311++G(3df,2p) and MP2/6-311++G(3df,2p) levels are given in Table 3. The final geometries, key hydrogen bond lengths, and the magnitude of $n(\text{O}) \rightarrow \sigma^*(\text{O}-\text{H})$ interactions of the phosphate and water complexes are given in Figure 8.

Hydration enthalpies show that H_2PO_4^- complexes are more stable than their PO_3^- counterparts when complexed with either two or three water molecules.^{3,12} The computed MP2/6-311++G(3df,2p) hydration enthalpies corrected for BSSE are within the reported 0.33 kcal/mol experimental uncertainty for PO_3^- and within the 1 kcal/mol uncertainty for H_2PO_4^- for the one- and two-water complexes. However, the predicted three-water PO_3^- complex hydration enthalpy is significantly lower than observed. The large difference between experimental and computed hydration enthalpies of PO_3^- with three water molecules has been a long-standing source of uncertainty and has been addressed elsewhere.^{7,8,12} Other factors beyond BSSE must be in operation. For example, it has been speculated that metaphosphate is involved in a reaction with water. As such, the experimental values reflect a mix of different structures. Even if BSSEs were included, the discrepancy between experimental and computed values would remain, since there is no way to include the mix of structures in this type of calculation.

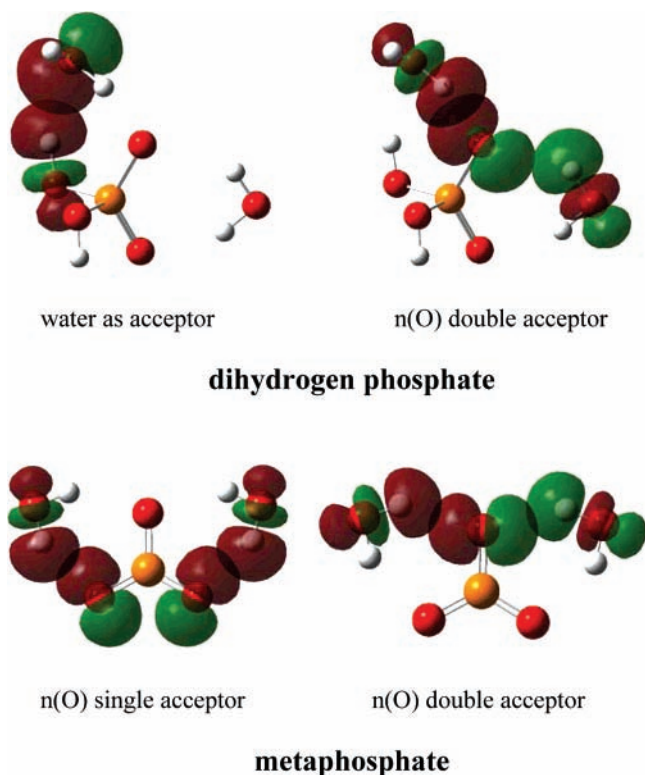


Figure 9. Important orbital interactions of metaphosphate and dihydrogen phosphate with two waters explaining the differences in hydrogen bond strengths. Oxygen is represented by the color red, phosphorus by orange, and hydrogen by white.

Consequently, the applied theory cannot accurately account for the hydration enthalpies.

To understand the underlying reason for the differences in hydration enthalpies, the hydrogen bonds formed by both PO_3^- and H_2PO_4^- were examined in detail. The main difference is that the hydrogen bonds formed between water and H_2PO_4^- are unequal in terms of geometry and strength as compared to those formed between water and PO_3^- . Unlike those of H_2PO_4^- , the hydrogen bonds in the two-water complex with PO_3^- are approximately equal in length (2.09–2.11 Å). The three-water complex with PO_3^- has uniform hydrogen-bonding distances at 2.13 Å. For all PO_3^- complexes considered, the waters behave as double hydrogen bond donors. In contrast, hydrogen bond lengths in H_2PO_4^- complexes can differ by as much as 0.46 Å. For example, in the two-water complex, **hp_2**, hydrogen bond lengths of 2.14, 2.01, and 1.68 Å are found. One water behaves as a double hydrogen bond donor, whereas the other water serves as a hydrogen bond donor and acceptor. In the three-water complex, **hp_3**, hydrogen bond lengths of 2.09, 2.02, and 1.70 Å are computed. In this case, one water behaves as a double hydrogen bond donor, whereas the other two waters serve as a simultaneous hydrogen bond donor and acceptor.

Interestingly, phosphate oxygens serve in three different capacities with water molecules. It may be a hydrogen bond acceptor for one donor, an acceptor for two simultaneous donors, or a hydrogen bond donor. In **mp_2**, two oxygens are acceptors for a single donor, whereas one oxygen is an acceptor for two hydrogen-bond-donating waters simultaneously. This difference in hydrogen-bonding responsibility explains the small differences computed in hydrogen bond lengths and charge transfer energies.

The oxygen coordinated with two hydrogen bond donors is a slightly weaker acceptor. As shown in Figure 9 (right-hand side) for the two-water complex with PO_3^- , a single lone pair

donates into two separate $\sigma^*(\text{O}-\text{H})$ orbitals, diluting the $n(\text{O})$ donor density, lowering the $n(\text{O})$ energy, and increasing the $n(\text{O})$ and $\sigma^*(\text{O}-\text{H})$ energy gap. Thus, less charge transfer (3.6 kcal/mol) and a longer hydrogen bond distance (2.11 Å) result, as compared to those of the oxygen with a single donor (4.0 kcal/mol and 2.09 Å) illustrated by the other PO_3^- structure in Figure 9 (left-hand side).

In **mp_3**, all of the phosphate oxygens are acceptors for two hydrogen-bond-donating waters simultaneously. Each PO_3^- oxygen atom has a single lone pair donating into two separate $\sigma^*(\text{O}-\text{H})$ orbitals (Figure 10), resulting in hydrogen bonds weaker than computed in the one- and two-water complexes for the same reasons stated above. As a consequence of the symmetry, all hydrogen bond lengths (2.13 Å) and charge-transfer energies (3.1 kcal/mol) are equivalent.

Dihydrogen phosphate exhibits different and more asymmetric hydrogen bonding. In the two- and three-water clusters (Figure 8), there is at least one water that serves as a double hydrogen bond donor. In **hp_2**, the same behavior as in the PO_3^- complex is observed, where the phosphoryl oxygen acceptor interacting with a single donor yields stronger hydrogen bonds (6.6 vs 3.2 kcal/mol) and shorter distances (2.01 vs 2.14 Å). The three-water case **hp_3** produces intermediate distances (2.09 Å) and energies (4.0 kcal/mol) for the formed double-donor, double-acceptor hydrogen bonds.

An interesting complex occurs when a water acts as both a hydrogen bond donor and a hydrogen bond acceptor, as found with **hp_2** and **hp_3**. These waters form hydrogen bonds of different strengths, even when the bonds originate from the same hydrogen bond acceptor atom. When the water is a simultaneous donor and acceptor, one hydrogen bond is extremely short (1.68 and 1.70 Å) between the water donor and oxygen acceptor. Short hydrogen bonds may be key to the observed stability differences between H_2PO_4^- and PO_3^- in two- and three-water complexes. The NBO method was used to examine the $n(\text{O}) \rightarrow \sigma^*(\text{O}-\text{H})$ interactions responsible for the short hydrogen bonds. $E(2)$ values corresponding to the respective $n(\text{O}) \rightarrow \sigma^*(\text{O}-\text{H})$ charge-transfer interactions are provided in Figure 8 in parentheses. It is noted that the short hydrogen bonds have extremely high $n(\text{O}) \rightarrow \sigma^*(\text{O}-\text{H})$ values of 30.7 and 27.6 kcal/mol. As previously discussed, these absolute charge transfer energies are likely overestimated; however, their relative values indicate that these hydrogen bonds are special and that improved orbital overlap or energies enhance the charge transfer or partial covalency.

The unusual strength of these short hydrogen bonds stems from the fact that the participating water molecule is also acting as a hydrogen bond acceptor. The NBO orbitals highlighting the different types of donor and acceptor interactions are given in Figures 9 and 10. Closer examination shows excellent $n(\text{O})$ and $\sigma^*(\text{O}-\text{H})$ alignment for cooperative charge transfer through a single water molecule (Figure 10, center and right-hand side). The withdrawal of electron density from the water molecule reduces the energy of the $\sigma^*(\text{O}-\text{H})$ orbital. As such, the computed $\sigma^*(\text{O}-\text{H})$ energy is 0.84 au, as compared to 0.88 au from the double-donor waters on PO_3^- and 0.90 au from the other water molecule on H_2PO_4^- . This lowering in energy of the $\sigma^*(\text{O}-\text{H})$ orbital reduces the energy gap between $n(\text{O})$ and $\sigma^*(\text{O}-\text{H})$ by 25.1 kcal/mol, yielding a stronger $n(\text{O}) \rightarrow \sigma^*(\text{O}-\text{H})$ charge transfer interaction and unusually short hydrogen bonds. Overall these findings explain the lack of stability between water and PO_3^- compared to H_2PO_4^- .

Biological Implications. Hydrogen bonds are a pervasive interaction in nature and common within enzyme active sites.^{75–78} How hydrogen bonding, especially short strong hydrogen bonds, impacts catalysis is an important biological

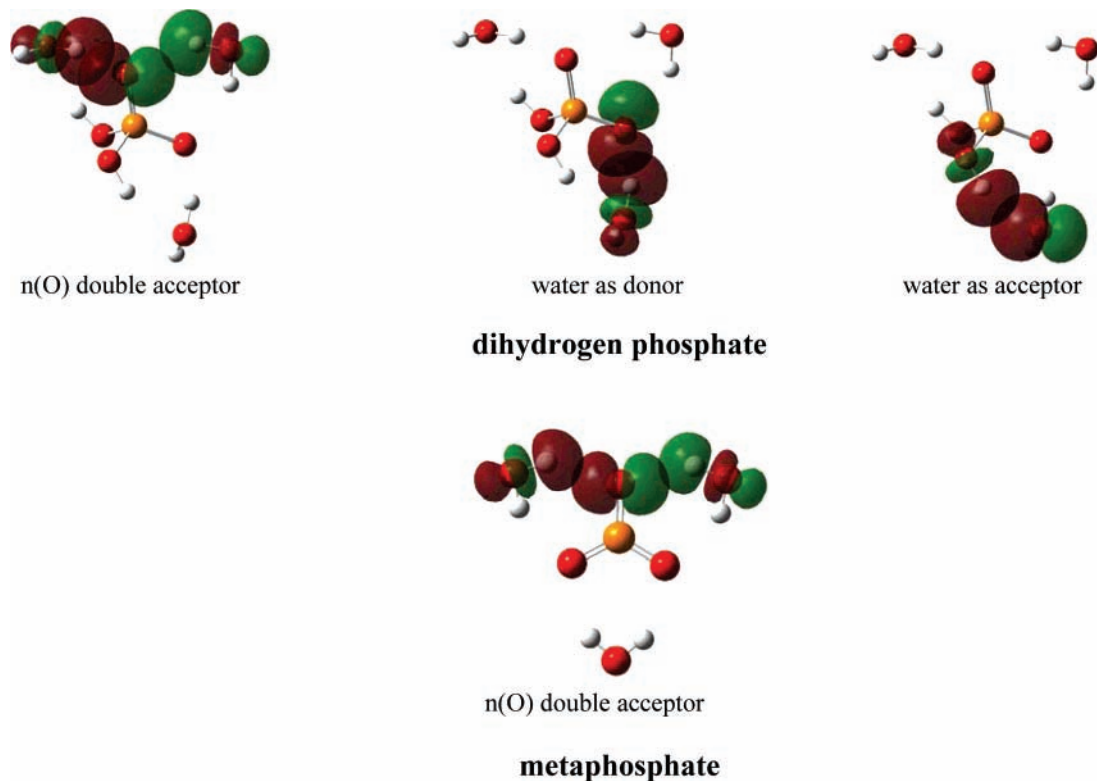


Figure 10. Important orbital interactions of metaphosphate and dihydrogen phosphate with three waters explaining the differences in hydrogen bond strengths. Oxygen is represented by the color red, phosphorus by orange, and hydrogen by white.

question that is actively studied.^{77–83} The role of this type of hydrogen bonding to enzyme catalysis is particularly interesting, since it has been proposed that such interactions can stabilize transition structures by 8 kcal/mol.⁷⁸ In this work for one-water complexes, it is shown that distal lone pairs of electrons can perturb orbital orientations and overlap, increase covalency through charge transfer, and modulate the strengths of hydrogen bonds. In complexes with more than one water, charge transfer can be reduced or greatly magnified depending on the hydrogen-bonding configuration. Since, configurational and conformational changes of phosphates are linked to the hydrogen bond strength, such changes during active site binding may be crucial to overall enzymatic activity or phosphoryl-transfer reactions. Although H_2PO_4^- is rare in enzymatic systems, other substituted phosphates, rich in lone pairs of electrons, may display the same connection between binding strength and conformational dependency. Future analysis of hydrogen bonding of phosphates in active sites with water, ions, or amino acids should include consideration of such stereoelectronic effects.

Conclusions

The electronic basis of hydrogen bonding of metaphosphate and dihydrogen phosphate with one to three waters was studied to understand the experimentally reported differences in enthalpies of hydration. The evaluation of the level of theory utilized shows that it is essential to employ basis set superposition error corrections along with supplemental diffuse functions to compute the enthalpy of hydration to experimental error for both metaphosphate and dihydrogen phosphate. Using natural bond orbital analysis, it is found that dihydrogen phosphate participates in stronger hydrogen bonding relative to metaphosphate due to greater hyperconjugative $n(\text{O}) \rightarrow \sigma^*(\text{O}-\text{H})$ interactions. The influence of subtle orbital interactions resulting from configurational and conformational changes is key to understanding the hydrogen-bonding differences between the

two phosphates. In the dihydrogen phosphate complex with one water, the repulsion between distal lone pairs and the $n(\text{O})$ donor orbital creates favorable orbital overlap between $n(\text{O})$ and $\sigma^*(\text{O}-\text{H})$, which increases the magnitude of charge transfer and consequently hydrogen bond strength relative to those of metaphosphate. In the two- and three-water complexes, the more asymmetric hydrogen-bonding configuration in dihydrogen phosphate allows for cooperative charge transfer that strengthens its hydrogen bond acceptor ability over that of PO_3^- . Waters in dihydrogen phosphate complexes serve as both a hydrogen bond donor and a hydrogen bond acceptor, which reduces the energy gap between $n(\text{O})$ and $\sigma^*(\text{O}-\text{H})$, leading to stronger hydrogen bonds. The connection among the phosphate conformation, orbital interactions, partial covalency, and hydration enthalpies has been demonstrated.

Acknowledgment. This work was funded in part by an American Heart Association (Florida, Puerto Rico affiliate) predoctoral fellowship (Grants 0415212B and 0615243B) to E.A.R. In addition, J.D.E. is grateful to the NSF and DoD (Grants CHE-0723109, CHE-0649182, CHE-0321147, CHE-0354052, CHE-0723109, and AAB/PSC CHE-030008P), Department of Education (Grants P116Z040100 and P116Z050331), and SGI Corp. and Gaussian Corp. for support of this work. We thank the Florida State University School of Computational Science and Information Technology (CSIT) for use of the IBM p-Series 690 Power3-based supercomputer and the IBM p-Series 690 Power4-based supercomputer.

Supporting Information Available: Gaussian archives for all structures at the B3LYP/6-311++G(3df,2p) and MP2/6-311++G(3df,2p) levels, Table S1, number of basis functions of PO_3^- and H_2PO_4^- and interaction enthalpies of the bifurcated complexes at the various levels of theory both with and without BSSE corrections, Table S2, covalent contribution to hydrogen-bonding interactions between metaphosphate and dihydrogen

phosphate (NBO energy values were calculated using the B3LYP/6-311++G(3df,2p) wave function on B3LYP/6-311++G(3df,2p)-optimized structures), the method for deletion optimizations, and relevant initial structures. This material is available free of charge via the Internet at <http://pubs.acs.org>.

References and Notes

- Butcher, W. W.; Westheimer, F. H. *J. Am. Chem. Soc.* **1955**, *77*, 2420.
- Bunton, C. A.; Llewellyn, D. R.; Oldham, K. G.; Vernon, C. A. *J. Chem. Soc.* **1958**, 3574.
- Keesee, R. G.; Castleman, A. W. *J. Am. Chem. Soc.* **1989**, *111*, 9015.
- Henchman, M.; Viggiano, A. A.; Paulson, J. F.; Freedman, A.; Wormhoudt, J. *J. Am. Chem. Soc.* **1984**, *107*, 1453.
- Harvan, D. J.; Hass, J. R.; Busch, K. L.; Burse, M. M.; Ramirez, F.; Meyerson, S. *J. Am. Chem. Soc.* **1979**, *101*, 7409.
- Choe, J.-Y.; Iancu, C. V.; Fromm, H. J.; Honzatko, R. B. *J. Biol. Chem.* **2003**, *278*, 16015.
- Ma, B.; Xie, Y.; Shen, M.; Schaefer, H. F. I. *J. Am. Chem. Soc.* **1993**, *115*, 1943.
- Wu, Y. D.; Houk, K. N. *J. Am. Chem. Soc.* **1993**, *115*, 11997.
- Range, K.; McGrath, M. J.; Lopez, X.; York, D. M. *J. Am. Chem. Soc.* **2004**, *126*, 1654.
- Buchwald, S. L.; Friedman, J. M.; Knowles, J., R. *J. Am. Chem. Soc.* **1984**, *106*, 4911.
- Calvo, K. C. *J. Am. Chem. Soc.* **1985**, *107*, 3690.
- Blades, A. T.; Ho, Y.; Kebarle, P. *J. Am. Chem. Soc.* **1996**, *118*, 196.
- Blades, A. T.; Ho, Y.; Kebarle, P. *J. Phys. Chem.* **1996**, *100*, 2443.
- Zhang, L.; Xie, D.; Xu, D.; Guo, H. *J. Phys. Chem. A* **2005**, *109*, 11295.
- Friedman, J. M.; Knowles, J. R. *J. Am. Chem. Soc.* **1985**, *107*, 6126.
- Lad, C.; Williams, N. H.; Wolfenden, R. *Proc. Natl. Acad. Sci. U.S.A.* **2003**, *100*, 5607.
- Voet, D.; Voet, J. G. *Biochemistry*, 2nd ed.; John Wiley: New York, 1995; p 428.
- Kropman, M. F.; Bakker, H. J. *Science* **2001**, *291*, 2118.
- Kropman, M. F.; Bakker, H. J. *J. Chem. Phys.* **2001**, *115*, 8942.
- Chandra, A. *J. Phys. Chem. B* **2003**, *107*, 3899.
- Thompson, W. H.; Hynes, J. T. *J. Am. Chem. Soc.* **2000**, *122*, 6278.
- Arnold, W. D.; Oldfield, E. *J. Am. Chem. Soc.* **2000**, *122*, 12835.
- Isaacs, E. D.; Shukla, A.; Platzman, P. M.; Hamann, D. R.; Barbiellini, B.; Tulk, C. A. *Phys. Rev. Lett.* **1999**, *82*, 600 LP.
- Fabiola, F.; Bertram, R.; Korostelev, A.; Chapman, M. S. *Protein Sci.* **2002**, *11*, 1415.
- Morozov, A. V.; Kortemme, T.; Tsemekhman, K.; Baker, D. *Proc. Natl. Acad. Sci. U.S.A.* **2004**, *101*, 6946.
- Wilkens, S. J.; Westler, W. M.; Weinhold, F.; Markley, J. L. *J. Am. Chem. Soc.* **2002**, *124*, 1190.
- Belair, S. D.; Hernandez, H.; Francisco, J. S. *J. Am. Chem. Soc.* **2004**, *126*, 3024.
- Alabugin, I. V.; Manoharan, M.; Peabody, S.; Weinhold, F. *J. Am. Chem. Soc.* **2003**, *125*, 5973.
- Parreira, R. L. T.; Galembeck, S. E. *J. Am. Chem. Soc.* **2003**, *125*, 15614.
- Weinhold, F.; Landis, C. *Valency and Bonding*; Cambridge University Press: Cambridge, U.K., 2005.
- Frisch, M. J.; Trucks, G. W.; Schlegel, H. B.; Scuseria, G. E.; Robb, M. A.; Cheeseman, J. R.; Montgomery, J. A., Jr.; Vreven, T.; Kudin, K. N.; Burant, J. C.; Millam, J. M.; Iyengar, S. S.; Tomasi, J.; Barone, V.; Mennucci, B.; Cossi, M.; Scalmani, G.; N. Rega; Petersson, G. A.; Nakatsuji, H.; Hada, M.; Ehara, M.; Toyota, K.; Fukuda, R.; Hasegawa, J.; Ishida, M.; Nakajima, T.; Honda, Y.; Kitao, O.; Nakai, H.; Klene, M.; Li, X.; Knox, J. E.; Hratchian, H. P.; Cross, J. B.; Adamo, C.; Jaramillo, J.; Gomperts, R.; Stratmann, R. E.; Yazyev, O.; Austin, A. J.; Cammi, R.; Pomelli, C.; Ochterski, J. W.; Ayala, P. Y.; Morokuma, K.; Voth, G. A.; Salvador, P.; Dannenberg, J. J.; Zakrzewski, V. G.; Dapprich, S.; Daniels, A. D.; Strain, M. C.; Farkas, O.; Malick, D. K.; Rabuck, A. D.; Raghavachari, K.; Foresman, J. B.; Ortiz, J. V.; Cui, Q.; Baboul, A. G.; Clifford, S.; Cioslowski, J.; Stefanov, B. B.; Liu, G.; Liashenko, A.; Piskorz, P.; Komaromi, I.; Martin, R. L.; Fox, D. J.; Keith, T.; Al-Laham, M. A.; Peng, C. Y.; Nanayakkara, A.; Challacombe, M.; Gill, P. M. W.; Johnson, B.; Chen, W.; Wong, M. W.; Gonzalez, C.; Pople, J. A. *Gaussian 03*, revision D.01; Gaussian Inc.: Pittsburgh, PA, 2003.
- Friesner, R. A.; Guallar, V. *Annu. Rev. Phys. Chem.* **2005**, *56*, 389.
- Møller, C.; Plesset, M. S. *Phys. Rev.* **1934**, *46*, 618.
- Becke, A. D. *Phys. Rev. A* **1988**, *38*, 3098.
- Becke, A. D. *J. Chem. Phys.* **1993**, *98*, 1372.
- Lee, C.; Yang, W.; Parr, R. G. *Phys. Rev. B* **1988**, *37*, 785.
- Tuma, C.; Sauer, J. *Phys. Chem. Chem. Phys.* **2006**, *8*, 3955.
- Antony, J.; Grimme, S. *Phys. Chem. Chem. Phys.* **2006**, *8*, 5287.
- Cybulski, S. M.; Seversen, C. E. *J. Chem. Phys.* **2005**, *122*, 014117.
- Clark, T.; Chandrasekhar, J.; Spitznagel, G. W.; Schleyer, P. v. R. *J. Comput. Chem.* **1983**, *4*, 294.
- Modelli, A.; Mussoni, L.; Fabbri, D. *J. Phys. Chem. A* **2006**, *110*, 6482.
- Stefanovich, E. V.; Boldyrev, A. I.; Truong, T. N.; Simons, J. *J. Phys. Chem. B* **1998**, *102*, 4205.
- Chou, P.-T.; Wei, C.-Y.; Hung, F.-T. *J. Phys. Chem. B* **1997**, *101*, 9119.
- Chattopadhyay, S.; Plummer, P. L. M. *Chem. Phys.* **1994**, *182*, 39.
- Plummer, P. L. M. *J. Phys. Chem. B* **2004**, *108*, 19582.
- Wong, M. W.; Wiberg, K. B.; Frisch, M. J. *J. Am. Chem. Soc.* **1992**, *114*, 1645.
- Binkley, J. S.; Pople, J. A.; Pietro, W. J.; Hehre, W. J. *J. Am. Chem. Soc.* **1982**, *104*, 2797.
- Hehre, W. J.; Ditchfield, R.; Pople, J. A. *J. Chem. Phys.* **1972**, *56*, 2257.
- Dill, J. D.; Pople, J. A. *J. Chem. Phys.* **1975**, *62*, 2921.
- Francl, M. M.; Pietro, W. J.; Hehre, W. J.; Binkley, J. S.; Gordon, M. S.; Defrees, D. J.; Pople, J. A. *J. Chem. Phys.* **1982**, *77*, 3654.
- Krishnan, R.; Binkley, J. S.; Seeger, R.; Pople, J. A. *J. Chem. Phys.* **1980**, *72*, 650.
- Kendall, R. A.; Dunning, T. H., Jr.; Harrison, R. J. *J. Chem. Phys.* **1992**, *96*, 6796.
- Woon, D. E.; Dunning, T. H. J. *J. Chem. Phys.* **1993**, *98*, 1358.
- Boys, S. F.; Bernardi, F. *Mol. Phys.* **1970**, *19*, 553.
- Kim, K. S.; Tarakeshwar, P.; Lee, J. Y. *Chem. Rev.* **2000**, *100*, 4145.
- Acevedo, O.; Evanseck, J. D. Transition States and Transition Structures. In *Computational Medicinal Chemistry for Drug Discovery*; Bultinck, P., De Winter, H., Langenaeker, W., Tollenaere, J. P., Dekker, M., Eds.; 2004; p 323.
- Glendening, E. D.; Badenhop, J. K.; Reed, A. E.; Carpenter, J. E.; Weinhold, F. NBO 3.1, 1996.
- Alabugin, I. V.; Zeidan, T. A. *J. Am. Chem. Soc.* **2002**, *124*, 3175.
- Alabugin, I. V.; Mariappan, M.; Zeidan, T. A. *J. Am. Chem. Soc.* **2003**, *125*, 14014.
- Dreuw, A.; Schweinsberg, H.; Cederbaum, L. S. *J. Phys. Chem. A* **2002**, *106*, 1406.
- Torrent-Sucarrat, M.; Sola, M.; Toro-Labbe, A. *J. Phys. Chem. A* **2006**, *110*, 8901.
- Kitaura, K.; Morokuma, K. *Int. J. Quantum Chem.* **1976**, *10*, 325.
- Mo, Y.; Peyerimhoff, S. D. *J. Chem. Phys.* **1998**, *109*, 1687.
- Mo, Y.; Zhang, Y.; Gao, J. *J. Am. Chem. Soc.* **1999**, *121*, 5737.
- Umeyama, H.; Morokuma, K. *J. Am. Chem. Soc.* **1977**, *99*, 1316.
- Reed, A. E.; Curtiss, L. A.; Weinhold, F. *Chem. Rev.* **1988**, *88*, 899.
- Glendening, E. D.; Streitwieser, A. *J. Chem. Phys.* **1994**, *100*, 2900.
- Mo, Y.; Gao, J. *Acc. Chem. Res.* **2007**, *40*, 113.
- Blades, A. T.; Klassen, J. S.; Kebarle, P. *J. Am. Chem. Soc.* **1996**, *118*, 12437.
- Del Bene, J. E.; Mettee, H. D.; Frisch, M. J.; Luke, B. T.; Pople, J. A. *J. Phys. Chem.* **1983**, *87*, 3279.
- Frisch, M. J.; Del Bene, J. E.; Raghavachari, K.; Pople, J. A. *Chem. Phys. Lett.* **1981**, *83*, 240.
- Freccero, M.; Di, Valentin, C.; Sarzi-Amade, M. *J. Am. Chem. Soc.* **2003**, *125*, 3544.
- Clark, T.; Chandrasekhar, J.; Spitznagel, G. W.; Schleyer, P. v. R. *J. Comput. Chem.* **1983**, *4*, 294.
- Pendas, A. M.; Blanco, M. A.; Francisco, E. *J. Chem. Phys.* **2006**, *125*, 184112.
- Zhou, G.; Somasundaram, T.; Blanc, E.; Parthasarathy, G.; Ellington, W. R.; Chapman, M. S. *Proc. Natl. Acad. Sci. U.S.A.* **1998**, *95*, 8449.
- Thomaeus, A.; Carlsson, J.; Aqvist, J.; Widersten, M. *Biochemistry* **2007**, *46*, 2466.
- Guthrie, J. P. *Chem. Biol.* **1996**, *3*, 163.
- Shan, S.; Herschlag, D. *J. Am. Chem. Soc.* **1996**, *118*, 5515.
- Williams, N. H. *Biochim. Biophys. Acta* **2004**, *1697*, 279.
- Perrin, C. L.; Nielson, J. B. *Annu. Rev. Phys. Chem.* **1997**, *48*, 511.
- Gerlt, J. A.; Kreevoy, M. M.; Cleland, W. W.; Frey, P. A. *Chem. Biol.* **1997**, *4*, 259.
- Cleland, W. W.; Frey, P. A.; Gerlt, J. A. *J. Biol. Chem.* **1998**, *273*, 25529.
- Czyryca, P. G.; Hengge, A. C. *Biochim. Biophys. Acta* **2001**, *1547*, 245.